Journal of Materials and Electronic Devices 2 (2024) 18-24

JOURNAL OF MATERIALS AND ELECTRONIC DEVICES
FYTRONIX JMED
http://dergi-fytronix.com/

Analyzing the Mechanical Properties of An Auxetic Structure Under Compression

Gülcan AYDIN*, Sait Eren SAN

Kocaeli University, Faculty of Arts and Sciences, Department of Physics, Kocaeli, Turkey

Auxetic metamaterials, with their unique mechanical traits and negative Poisson's ratios, offer a promising path in material innovation. This study employs finite element analysis to delve into the mechanical dynamics of auxetic metamaterials, particularly focusing on re-entrant lattice structures. By investigating geometric array configurations, unit cell sizes, and thicknesses, it examines their impact on displacement, strain, von Mises stress, and Young's modulus. Meticulous numerical simulations reveal significant correlations between these parameters and structural integrity. These findings highlight the critical role of geometric arrangement, unit cell dimensions, and thickness in optimizing the design and performance of auxetic metamaterials across various engineering fields. By enhancing our understanding and offering valuable insights, this research advances the development and application of auxetic metamaterials.

Keywords: *Metamaterial; Re-Entrant Lattice; Mechanical Properties; Finite Element Analysis*
Submission Date: 18 March 2024
Acceptance Date: 01 June 2024

**Corresponding author: gulcan.aydin@kocaeli.edu.tr*

1. Introduction

Rapid advancements in engineering and materials science have opened new frontiers in material design. Auxetic metamaterials, known for their unique mechanical properties, exemplify these innovations. Unlike traditional materials, auxetic metamaterials expand when stretched due to their negative Poisson ratios, making them ideal for energy absorption and impact resistance.

These materials offer exceptional design flexibility and customization. Their mechanical properties can be precisely tailored, promoting innovation in various fields. Key features include elastic modulation, high energy absorption, shape memory, and the ability to revert to their original shape after deformation. Such attributes are particularly valuable in medical devices, sensors, and actuators.

This study involves the finite element analysis of auxetic metamaterials designed using re-entrant unit topology. By altering geometric arrays, unit cell thicknesses, and unit cell dimensions, the maximum stress, deformation, and Young's modulus were examined. These analyses provide valuable insights into material design and performance understanding.

2. Overview of Auxetic Structures: Properties and Applications

2.1. What is an auxetic structure?

An auxetic structure is a material with a negative Poisson's ratio [1-2]. While most natural materials exhibit a positive Poisson's ratio, auxetic structures have unique properties due to this feature.

The term 'auxetic' originates from the Greek word "Auxetos," meaning to increase, and was first coined by Evans in 1991 [3]. The Poisson ratio of isotropic materials is typically a maximum of +0.5. For solid, homogeneous isotropic materials, the maximum negative Poisson's ratio is -1. Anisotropic materials can exceed this limit [3-5].

Poisson's ratio illustrates how a material responds to mechanical force. It is defined as the negative ratio of transverse strain to axial strain in the elastic loading region. This ratio indicates how much a material contracts when

subjected to a tensile force. Depending on the material, Poisson's ratio can be positive, zero, or negative.

Materials with a positive Poisson's ratio increases in tension in the direction of the applied force, causing a decrease in axial strain. Conversely, when compressive force is applied, strain decreases in the direction of the applied force and increases perpendicularly.

Materials with a negative Poisson's ratio expands in both directions when subjected to tensile force and contract when compressed. Additionally, these materials take on a dome-like shape when bent.

Auxetic materials are often referred to as smart materials due to their unique properties, including:

- Excellent energy absorption [6].
- High fracture toughness.
- Tailorable mechanical properties [7].
- Unique deformation mechanisms.
- Shape memory.
- High shear modulus.
- High indentation resistance.
- Improved acoustic properties.

Applications of auxetic materials span various industries, including biomedical, construction, automotive, aerospace, textiles, security, and sensors. These materials are widely utilized in the production of curved-bodied products. They are used in functional composite materials and sensor and actuator systems. In biomedical applications, they can be used in prosthetics, skeletal tissues, stents, implants, and suture anchors.

2.2. A Historical overview of auxetic materials

The exploration of auxetic materials dates to the early 1900s, initiated by Woldemar Voigt. Through investigations on iron pyrite, Voigt achieved a negative Poisson ratio of -0.14. Although Voigt attributed this behaviour to crystal twinning, a precise explanation remained elusive.

In 1927, A.E.H. Love produced an auxetic material with a Poisson ratio of -0.14 using cubic crystal pyrite [8]. Subsequently, in 1982, Gibson and colleagues elucidated that auxetic behaviour arises from the bending of ribs in a silicone rubber honeycomb structure [9].

Analytically examining re-entrant auxetic structures in 1985, Almgren contributed to the understanding of these materials [10]. Roderick Lakes pioneered the production of auxetic foam in 1987, utilizing three-axis volumetric compression for open-cell auxetic polyurethane foams. This was followed by heat treatment, resulting in a Poisson ratio of -0.7. The three-axis compression altered the original cellular microstructure to a more random configuration, and subsequent heating and cooling processes stabilized this new geometry. This methodology led to the creation of foams with negative Poisson ratios [11-13].

Throughout the late 1980s, Evans and Caddock extensively researched the production of polymer auxetic structures. They observed auxetic behaviour in nodular-fibril structures of polytetrafluoroethylene (PTFE), demonstrating a negative Poisson ratio of -12 [14]. Evans and Alderson developed ultra-high molecular weight polyethylene (UHMWPE) with a nodular-fibril microstructure like that of PTFE. They subjected this material to compression and subsequent sintering, achieving a Poisson ratio of -19 compared to traditional polyethylene [15].

Following Lakes' pioneering work, numerous studies ensued, expanding the application areas of auxetic materials. Auxetic materials are categorized as natural and synthetic. Man-made auxetic materials include metals, ceramics, composites, polymers, laminates, and fibres [2, 15-18].

Auxetic materials are designed and produced based on their geometric features and deformation mechanisms [20]. In recent years, a plethora of artificial auxetic structures with diverse geometric configurations have been designed and modelled. The most frequently utilized geometric structures in the literature include 2D and 3D re-entrant structures, the lost rib model, chiral structures, rotating units, and star-shaped units. These unique unit cells, repetitively arranged within structures, create auxetic materials. These structures, observable at both the molecular and macro levels, offer versatile applications. Additionally, irregular structures outside these categories have also been explored [21].

The production of auxetic foams with re-entrant structures was first accomplished by Lakes in 1978, utilizing polyurethane material [17]. In the literature, auxetic foams have been produced using various materials such as polyester urethane, silicone rubber, and copper.

In summary, the historical evolution of auxetic materials demonstrates a continuous exploration and development process, leading to diverse applications and classifications in both natural and synthetic realms.

3. Simulation Details

In this study, numerical simulation was employed to investigate the behaviour of Re-Entrant lattice structures under compressive loading.

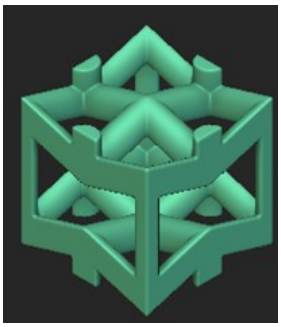

Figure 1: Re-entrant unit cell is shown.

The study included a static structural analysis, where cubic lattices were meticulously evaluated based on their performance in terms of maximum stress and deformation

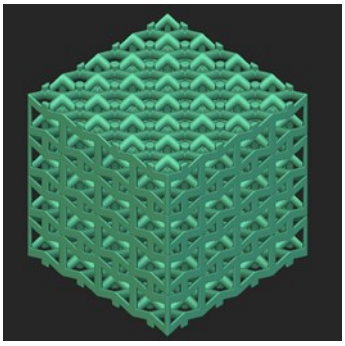

Figure 2: Cubic lattice is shown.

The primary focus was to discern the impact of lattice structure geometry, unit cell size, and unit cell thickness on both maximum stress and deformation. To achieve this, the geometric array was systematically altered to include configurations of 1x1x1, 2x2x2, 3x3x3, and 4x4x4. Throughout this process, a consistent unit cell size of 2 mm and a fixed thickness of 1 mm were maintained.

Next, the investigation explored the effects of varying unit cell sizes within the lattice structure on both maximum stress and deformation. This entailed adjusting the unit cell size randomly between 0.2 mm and 5 mm, while keeping the thickness constant at 1 mm. The lattice volume was set at 20x20x20 mm.

Finally, the study examined the influence of changes in unit cell thickness within the lattice structure on both maximum stress and deformation, with the unit cell size held constant at 2 mm.

Inconel 625, with a Young's modulus of 200 GPa, was selected for this investigation due to its specific properties and suitability for the intended application.

The lattice structures were designed using nTopology® software. Each structure consisted of two plates interconnected by a lattice framework, with the top and bottom plates strategically positioned to encapsulate the lattice. The top plate of each lattice structure was subjected to a uniformly applied force of 1000 N, while the bottom plate was constrained in all directions.

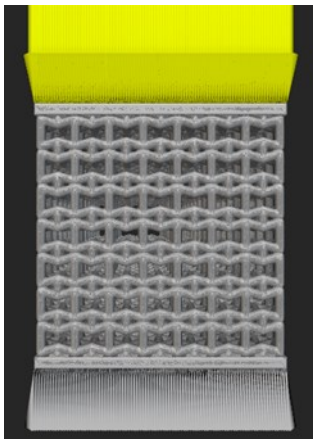

Figure 3: The upper plate of the Lattice structure is shown to be subjected to a uniformly applied force of 1000 N, while the lower plate is constrained in all directions.

In the nTopology® software (Student Version), a volumetric finite element mesh of the entire lattice structure was generated, and the lattice structures were created as solid elements. The connectivity between the plates and the lattice was facilitated through nodal joints.

Additionally, a tetrahedral mesh with element sizes as small as 0.25 mm was utilized to ensure the accuracy and reliability of the finite element analysis.

4. Result and Discussion

4.1. Influence of Unit Cell Configurations

This study has yielded significant findings by employing numerical simulation to investigate the characteristics of Re-Entrant lattice structures. The primary focus was to determine the effect of different geometric array sizes (1x1x1, 2x2x2, 3x3x3, and 4x4x4) on the mechanical properties of these structures.

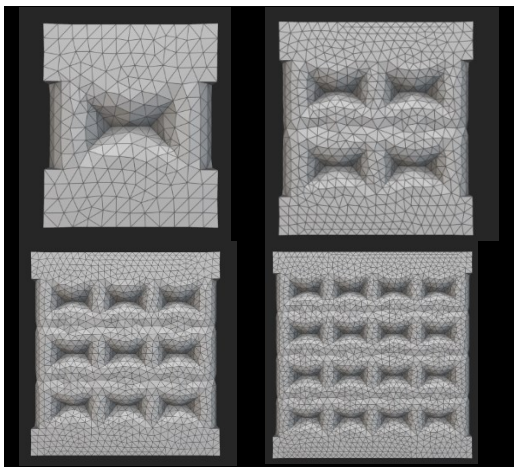

Figure 4: Geometric array dimensions (1x1x1, 2x2x2, 3x3x3 and 4x4x4) are shown.

The mechanical behaviour of the structures was examined under varying geometry array configurations, ranging from 1x1x1 to 4x4x4, while subjected to a 1000 N load.

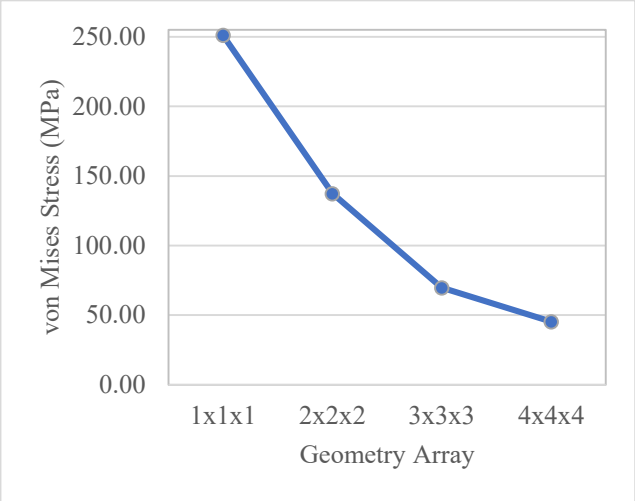

Figure 5: Effect of changing geometry array on von Mises Stress.

Table 1: The effect of changing geometry array on mechanical properties was examined.

Geometry Array	Displacement (mm)	Strain	von Mises Stress (MPa)	Young Modulus (GPa)
1x1x1	0,00223	0,00045	251.0	561
2x2x2	0,00140	0,00022	137.3	636
3x3x3	0,00103	0,00012	69.73	603
4x4x4	0,00081	0,00007	45.33	615

The following observations were made:

The displacement of the structure decreased as the geometry array size increased. For instance, with a 1x1x1 configuration, the displacement was 0.002234 mm, whereas with a 4x4x4 configuration, it decreased to 0.0008104 mm. Similar to displacement, the strain experienced by the structure also decreased with larger geometry array configurations. At a 1x1x1 configuration, the strain was 0.000447, while at a 4x4x4 configuration, it reduced to 0.00007362.

The von Mises stress values exhibited a decreasing trend as the geometry array size increased. At a 1x1x1 configuration, the stress Von Misses was 251.0 MPa, while at a 4x4x4 configuration, it decreased to 45.33 MPa.

The Young Modulus showed a slight variation with different geometry array configurations. However, no clear trend was observed in its behaviour with changes in geometry array size.

These results indicate the significant influence of geometry array configurations on the mechanical properties of the structure. Understanding these relationships is crucial for optimizing the design and performance of such structures in various engineering applications. Specifically, the findings suggest that larger geometric array sizes result in lower maximum stress and more homogeneous mechanical properties.

4.2. Effect of the Unit Cell Size

The mechanical response of the re-entrant lattice structures was examined under various unit cell sizes, ranging from 0.2 mm to 5 mm, while subjecting the structure to a 1000 N load on the top plate.

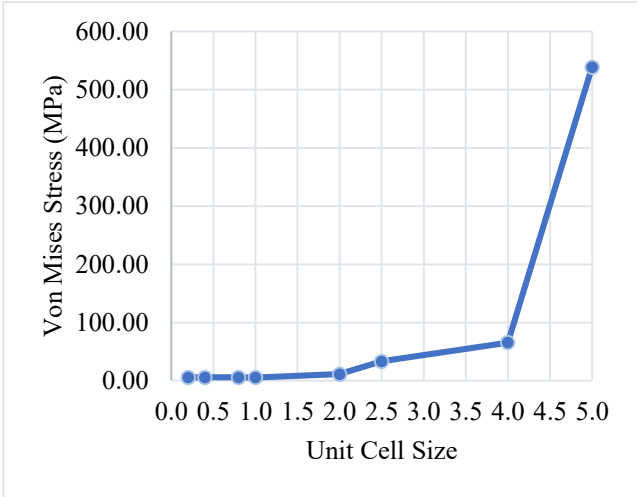

Figure 6: Effect of changing unit cell size array on von Mises Stress

Table 2: The effect of changing unit cell size on mechanical properties was examined.

Unit Cell Size (mm)	Displacement (mm)	Strain	von Mises Stress (MPa)	Young Modulus (GPa)
0.2	0.000241719	0.00000742711	5.88799	792,770
0.4	0.000241769	0.00000740890	5.81485	784,847
0.8	0.000242478	0.00000750902	5.82879	776,238
1	0.000242939	0.00000758945	5.73413	755,540
2	0.000361141	0.0000172027	11.4329	664,599
2.5	0.00103682	0.0000875197	33.4262	381,928
4	0.00335574	0.0000971626	65.2007	671,047
5	0.00658898	0.000915365	538.626	588,428

The following observations were made:

As the unit cell size increased, the displacement of the structure also increased. Smaller unit cell sizes exhibited minimal displacement, while larger unit cell sizes resulted in more significant displacements. For example, at a unit cell size of 0.2 mm, the displacement was 0.000241719 mm,

whereas at a unit cell size of 5 mm, the displacement increased to 0.00658898 mm.

Like displacement, the strain experienced by the structure increased with larger unit cell sizes. Smaller unit cell sizes corresponded to lower strain values, while larger unit cell sizes led to higher strain values. For instance, at a unit cell size of 0.2 mm, the strain was 0.00000742711 mm, whereas at a unit cell size of 5 mm, the strain increased to 0.000915365 mm.

The von Mises stress, representing the maximum equivalent stress experienced by the structure, also varied with unit cell size. Larger unit cell sizes resulted in higher von Mises stress values, indicating increased stress concentrations within the structure. At a unit cell size of 0.2 mm, the von Mises stress was 5.88799 MPa, while at a unit cell size of 5 mm, it rose to 538.626 MPa.

The Young's Modulus, representing the material's stiffness, showed an inverse relationship with unit cell size. Smaller unit cell sizes exhibited higher Young's Modulus values, reflecting a stiffer material response, whereas larger unit cell sizes exhibited lower Young's Modulus values, indicating a more compliant material behaviour.

Overall, these results highlight the significant influence of unit cell size on the mechanical properties of re-entrant lattice structures.

4.3. Effect of the Unit Cell Thickness

The mechanical properties of the structure were examined under varying unit cell thicknesses, ranging from 0.4 mm to 1 mm.

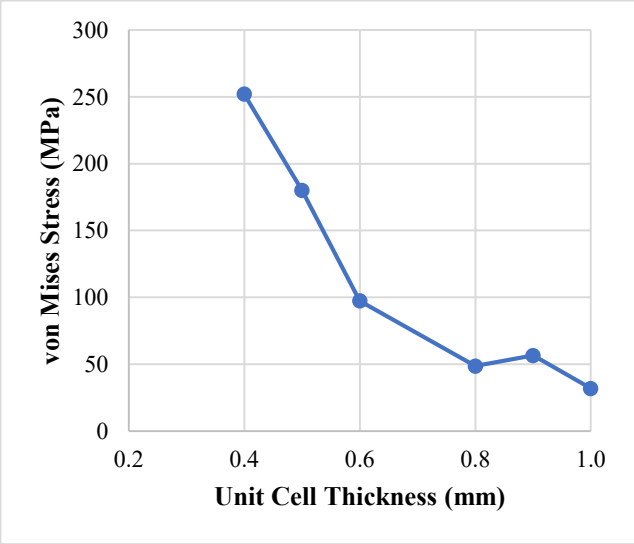

Figure 7: Effect of changing unit cell thickness array on von Mises Stress

Table 3: The effect of changing unit cell thickness on mechanical properties was examined.

Unit Cell Thickness (mm)	Displacement (mm)	Strain	von Mises Stress (MPa)	Young Modulus (GPa)
0.4	0.0387	0.000964	252.0	261
0.5	0.0181	0.000513	180.0	352
0.6	0.00582	0.000193	97.4	506
0.8	0.00262	0.000075	48.7	653
0.9	0.00193	0.000231	56.6	245
1	0.00148	0.000050	31.9	632

The structure was subjected to a load, and the following observations were made:

Increasing unit cell thickness resulted in a decrease in displacement. For instance, as the unit cell thickness increased from 0.4 mm to 1 mm, the displacement decreased from 0.0387 mm to 0.00148 mm.

Similarly, unit cell thickness showed an inverse relationship with strain. Thicker unit cell thicknesses corresponded to lower strain values. For example, at a unit cell thickness of 0.4 mm, the strain was 0.000964, whereas at a thickness of 1 mm, the strain decreased to 0.0000505.

The von Mises stress values decreased as the unit cell thickness increased. At a thickness of 0.4 mm, the von Mises stress was 252.0 MPa, while at a thickness of 1 mm, it reduced to 31.9 MPa.

Although there was some variability, no clear trend was observed between unit cell thickness and Young's Modulus. The values showed fluctuations across different thicknesses.

5. Conclusion

In this comprehensive study, the mechanical properties of Re-Entrant lattice structures were thoroughly investigated through finite element analysis, focusing on geometric array configurations, unit cell sizes, and unit cell thicknesses. The primary objective was to discern their influence on maximum stress, deformation, and Young's Modulus, crucial for optimizing material design and performance across various engineering applications.

Geometric Array Configurations: The analysis revealed a substantial impact of geometric array configurations on the mechanical properties of the lattice structures. As the geometry array size increased, displacements and strains decreased, while von Mises stress values exhibited a decreasing trend. Understanding these relationships is paramount for tailoring lattice structures to specific engineering requirements, ensuring enhanced performance and durability.

Unit Cell Sizes: The investigation into unit cell sizes demonstrated their significant influence on the mechanical behaviour of the structures. Larger unit cell sizes resulted in increased displacements, strains, and von Mises stress values, indicating a more compliant material response. Conversely, smaller unit cell sizes exhibited minimal

displacements and strains, coupled with higher stress concentrations. This understanding facilitates precise control over material stiffness and deformation characteristics, crucial for diverse engineering applications.

Unit Cell Thicknesses: The study elucidated the impact of unit cell thicknesses on structural performance, revealing a notable decrease in displacements and strains with increasing thickness. Thicker unit cell thicknesses correlated with reduced von Mises stress values, indicative of enhanced structural integrity and resistance to mechanical loads. Although fluctuations were observed in Young's Modulus across different thicknesses, no clear trend emerged, highlighting the complexity of the relationship between unit cell thickness and material stiffness.

Implications for Material Design: These findings underscore the importance of meticulous consideration of geometric array configurations, unit cell sizes, and unit cell thicknesses in the design and optimization of Re-Entrant lattice structures. By leveraging this knowledge, engineers and material scientists can tailor material properties to specific application requirements, ranging from energy absorption and impact resilience to medical devices and aerospace components. Moreover, the insights garnered from this study contribute to the broader understanding of auxetic metamaterials, fostering continued innovation and advancement in material design and engineering.

In conclusion, this research represents a significant step towards unlocking the full potential of auxetic metamaterials, paving the way for groundbreaking developments in diverse industrial sectors and scientific endeavours.

References

[1] A. Bezazi and F. Scarpa, Tensile fatigue of conventional and negative Poisson's ratio open cell PU foams, *Int J Fatigue*, vol. 31, no. 3, (2009), doi: 10.1016/j.ijfatigue.2008.05.005.

[2] R. Critchley, I. Corni, J. A. Wharton, F. C. Walsh, R. J. K. Wood, and K. R. Stokes, A review of the manufacture, mechanical properties and potential applications of auxetic foams, *Phys Status Solidi B Basic Res*, vol. 250, no. 10, (2013), doi: 10.1002/pssb.201248550.

[3] K. E. Evans, Auxetic polymers: a new range of materials, *Endeavour*, vol. 15, no. 4, (1991), doi: 10.1016/0160-9327(91)90123-S.

[4] R. Lakes, Negative Poisson's ratio materials," *Science*, vol. 238, no. 4826. (1987). doi: 10.1126/science.238.4826.551-a.

[5] Y. C. Fung, *Foundations of solid mechanics*. Prentice-Hall, (1968).

[6] F. Scarpa, L. G. Ciffo, and J. R. Yates, Dynamic properties of high structural integrity auxetic open cell foam, *Smart Mater Struct*, vol. 13, no. 1, (2004), doi: 10.1088/0964-1726/13/1/006.

[7] Y. Zhu, S. Jiang, Q. Zhang, J. Li, C. Yu, and C. Zhang, "A novel monoclinic auxetic metamaterial with tunable mechanical properties," *Int J Mech Sci*, vol. 236, (2022), doi: 10.1016/j.ijmecsci.2022.107750.

[8] A. E. H. Love, *Treatise on mathematical theory of elasticity. 4th edition*. (1944).

[9] L. J. Gibson, M. F. Ashby, G. S. Schajer, and C. I. Robertson, Mechanics of Two-Dimensional Cellular Materials., *Proc R Soc Lond A Math Phys Sci*, vol. 382, no. 1782, (1982), doi: 10.1098/rspa.1982.0087.

[10] Robert Almgren, An isotropic three-dimensional structure with Poisson's ratio =-1, *J Elast*, vol. 15, no. 4, (1985), doi: 10.1007/BF00042531.

[11] H. Jin and J. L. Lewis, Determination of Poisson's Ratio of Articular Cartilage by Indentation Using Different-Sized Indenters, *J Biomech Eng*, vol. 126, no. 2, (2004), doi: 10.1115/1.1688772.

[12] R. Lakes, No contractile obligations, *Nature*, vol. 358, no. 6389. (1992). doi: 10.1038/358713a0.

[13] R. Lakes, Foam structures with a negative poisson's ratio, *Science,* vol. 235, no. 4792, (1987), doi: 10.1126/science.235.4792.1038.

[14] B. D. Caddock and K. E. Evans, Microporous materials with negative Poisson's ratios. I. Microstructure and mechanical properties, *J Phys D Appl Phys*, vol. 22, no. 12, (1989), doi: 10.1088/0022-3727/22/12/012.

[15] K. L. Alderson and K. E. Evans, The fabrication of microporous polyethylene having a negative Poisson's ratio, *Polymer (Guildf)*, vol. 33, no. 20, (1992), doi: 10.1016/0032-3861(92)90294-7.

[16] T. Strek, B. Maruszewski, J. W. Narojczyk, and K. W. Wojciechowski, Finite element analysis of auxetic plate deformation, *J Non Cryst Solids*, vol. 354, no. 35–39, (2008), doi: 10.1016/j.jnoncrysol.2008.06.087.

[17] K. E. Evans and A. Alderson, Auxetic materials: Functional materials and structures from lateral thinking! *Advanced Materials*, vol. 12, no. 9, (2000), doi:10.1002/(SICI)1521-4095(200005)12:9%3C617::AID-ADMA617%3E3.0.CO;2-3

[18] A. Andersson, S. Lundmark, A. Magnusson, and F. H. J. Maurer, Shear behavior of flexible polyurethane foams under uniaxial compression, *J Appl Polym Sci*, vol. 111, no. 5, (2009), doi: 10.1002/app.29244.

[19] N. Ravirala, A. Alderson, and K. L. Alderson, Interlocking hexagons model for auxetic behaviour, *J Mater Sci*, vol. 42, no. 17, (2007), doi: 10.1007/s10853-007-1583-0.

[20] J. N. Grima, E. Manicaro, and D. Attard, Auxetic behaviour from connected different-sized squares and rectangles, in *Proceedings of the Royal Society A: Mathematical, Physical and Engineering Sciences*, (2011). doi: 10.1098/rspa.2010.0171.

[21] K. L. Alderson, A. Fitzgerald, and K. E. Evans, The strain dependent indentation resilience of auxetic

microporous polyethylene, *J Mater Sci*, vol. 35, no. 16, (2000), doi: 10.1023/A:1004830103411.